

Application of dopant segregation to metal-germanium-metal photodetectors and its dark current suppression mechanism

H. Zang, S. J. Lee, W. Y. Loh, J. Wang, M. B. Yu et al.

Citation: *Appl. Phys. Lett.* **92**, 051110 (2008); doi: 10.1063/1.2841061

View online: <http://dx.doi.org/10.1063/1.2841061>

View Table of Contents: <http://apl.aip.org/resource/1/APPLAB/v92/i5>

Published by the [American Institute of Physics](#).

Additional information on *Appl. Phys. Lett.*

Journal Homepage: <http://apl.aip.org/>

Journal Information: http://apl.aip.org/about/about_the_journal

Top downloads: http://apl.aip.org/features/most_downloaded

Information for Authors: <http://apl.aip.org/authors>

ADVERTISEMENT



Goodfellow
metals • ceramics • polymers • composites
70,000 products
450 different materials
small quantities fast

www.goodfellowusa.com

Application of dopant segregation to metal-germanium-metal photodetectors and its dark current suppression mechanism

H. Zang,^{1,2} S. J. Lee,^{2,a)} W. Y. Loh,¹ J. Wang,¹ M. B. Yu,¹ G. Q. Lo,¹ D. L. Kwong,¹ and B. J. Cho²

¹Institute of Microelectronics, A*STAR, 11 Science Park Road, Singapore 117685 Singapore

²Silicon Nano Devices Laboratory, ECE Department, National University of Singapore, Singapore 117576, Singapore

(Received 16 December 2007; accepted 17 January 2007; published online 6 February 2008)

We report the mechanism of dopant-segregation (DS) technique as applied in metal-germanium-metal photodetectors (MGM-PDs) for dark current suppression. Photodetectors with various dopant-segregation strategies were designed, fabricated, and characterized. Results show that asymmetric MGM-PD, with *n*- and *p*-type dopants segregated separately in two NiGe electrodes, is the optimized scheme in terms of dark current and responsivity. It shows a dark current of 10^{-6} A at -1 V, which is two to three orders of magnitude lower than that of MGM-PD without DS. *n*-type dopant (As) segregation in NiGe barrier increases the hole Schottky barrier height to 0.5 eV and, thus, plays a crucial role in dark current suppression. © 2008 American Institute of Physics. [DOI: 10.1063/1.2841061]

Heteroepitaxial Ge on Si provides an alternative solution for near-infrared photodetection for its low cost, process simplicity, and its compatibility with metal-oxide-semiconductor field effect transistor. Ge photodetectors on Si substrate have been demonstrated successfully¹⁻⁴ with high quality Ge epitaxial layer achieved using two-step Ge growth method.⁵ Metal-semiconductor-metal photodetector (MSM-PD) is a promising candidate for optoelectronic integrated circuit due to its ease of fabrication, low detector capacitance, and large device bandwidth.^{4,6,7} Nonetheless, the excessive dark current of MSM-PDs results in extra power consumption.

In MGM-PDs, Schottky barrier height (SBH) scaling due to the narrow band gap and strong Fermi-level pinning of metal/Ge interface at valence band further degrades the dark current.⁶ Several techniques were proposed for dark current suppression, such as amorphous Ge SBH enhancement layers,⁴ asymmetric area electrodes,⁷ and asymmetric metal electrodes.⁶ Recently, dopant segregation (DS) during silicidation technique had been successfully introduced into Schottky barrier-metal-oxide semiconductor field effect transistors (SB-MOSFETs), with demonstration of a significant improvement in drivability and off-state leakage current.^{8,9}

In this paper, we demonstrate an effective SBH engineering using the DS technique in MGM-PDs for dark current suppression. Along with the discussion on the dark current suppression mechanism, the effects of different DS strategies on the PD's electrical and optical behaviors are investigated.

Devices were fabricated on 8 in. *p*-type Si (100) wafer. First, the windows through a SiO₂ layer (120 nm) were opened for subsequent selective Ge epigrowth. High quality Ge epilayer (300 nm) was achieved by the two-step growth method combining with an intermediate ultrathin SiGe buffer (25 nm) in ultrahigh vacuum epichamber. The details can be found in Ref. 10. Ge was patterned and then implanted with arsenic (As: 1×10^{15} cm⁻²/12 keV) and boron (B: 1×10^{15} cm⁻²/12 keV) in the PD electrode regions for DS

contact formation. Four DS schemes for MGM-PDs were designed and fabricated on the same wafer for fair comparison. The DS split is described in the caption of Fig. 1. For the np-DS configuration, the outer electrode is implanted with B, while the inner electrode was implanted with As for the *n*-type electrode. After SiO₂ deposition, patterning, and contact hole etching, 25 nm Ni was deposited by sputtering for DS-NiGe electrode formation. Germanidation was carried out by rapid thermal annealing at 350 °C. Energy dispersive spectroscopy analysis on the Ni-germanide shows formation of mono-nickel germanide (NiGe). Unreacted Ni was removed by diluted nitric acid. Finally, Al metallization was performed. Figure 1 shows the schematic diagram of cross section of MGM-PD with 17 μm spacing between two electrodes.

Secondary-ion-mass spectroscopy (SIMS) has been employed to evaluate the DS effect in germanium substrate. From SIMS depth profiles of As and B in NiGe/Ge interfaces, it was observed that both As and B atoms were segregated around the interfaces of NiGe/Ge (e.g., As ~4

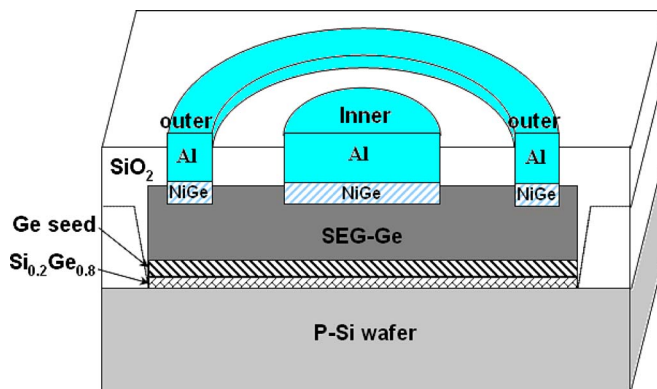


FIG. 1. (Color online) Schematic diagram of cross section of MGM-PD (inner electrodes width: 205 μm; outer electrodes width: 315 μm). DS schemes for MGM-PDs: (1) non-DS (with no DS in both inner and outer electrodes), (2) pp-DS (with B DS in both inner and outer electrodes), (3) np-DS (with As DS in inner electrode and B DS in outer electrode), and (4) nn-DS (with As DS in both inner and outer electrodes).

^{a)} Author to whom correspondence should be addressed. Electronic mail: elelsj@nus.edu.sg.

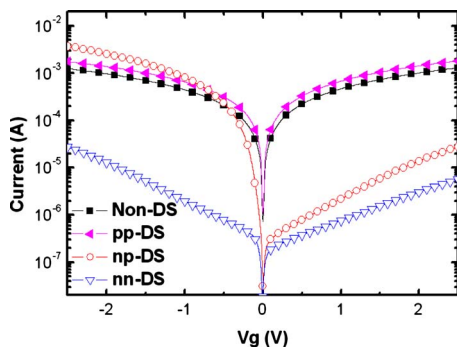


FIG. 2. (Color online) Dark current comparison between MGM-PDs with different DS strategies.

$\times 10^{18} \text{ cm}^{-3}$ and $B \sim 3 \times 10^{19} \text{ cm}^{-3}$). The implanted region was fully consumed by NiGe during germanidation, so the profiles of dopant atoms near the interface were determined only by the segregation effect.⁹ Figure 2 shows the dark current performances of MGM-PDs with different DS structures in the NiGe contact electrodes. The outer electrode is grounded for all electrical characterization, while a bias is applied to the inner electrode. Figure 3 shows the schematic of conduction and valence band profile in DS-MGM-PD with/without DS in two NiGe electrodes at positive biased condition. The two major components of dark current are carrier injection over the Schottky barrier (SB) (I_1 and I_2) and current associated with the thermally generated electron-hole pairs (I_3 and I_4). Since the epi-Ge has a threading dislocation of about 10^7 cm^{-2} ,¹⁰ I_3 and I_4 are also considerable components to dark current. In MGM-PD without DS technique, as shown in Fig. 3(a), due to the Fermi-level pinning effect between NiGe and Ge, hole SBH is about 0.07–0.1 eV in NiGe/*p*-Ge and electron SBH is about 0.6 eV in NiGe/*n*-Ge.^{9,11} The major component of the dark current is the hole injection over the SB (I_1). The MGM-PD without DS shows a high dark current of $4 \times 10^{-4} \text{ A}$ at 1 V (Fig. 2). In pp-DS-MGM-PD, B segregated in NiGe/Ge interface causes an abrupt band bending upward, resulting in the re-

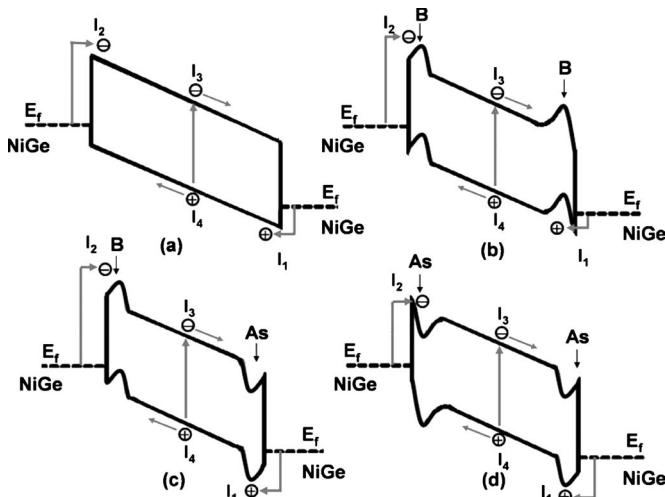


FIG. 3. Schematic conduction and valence band profile in DS-MGM-PD with/without dopant segregation in two NiGe electrodes at positive bias for (a) MGM-PD without DS (non-DS), (b) MGM-PD with B segregation in two electrodes (pp-DS), (c) MGM-PD with B and As segregated separately in two NiGe electrodes (np-DS), and (d) MGM-PD with As segregation in two electrodes (nn-DS).

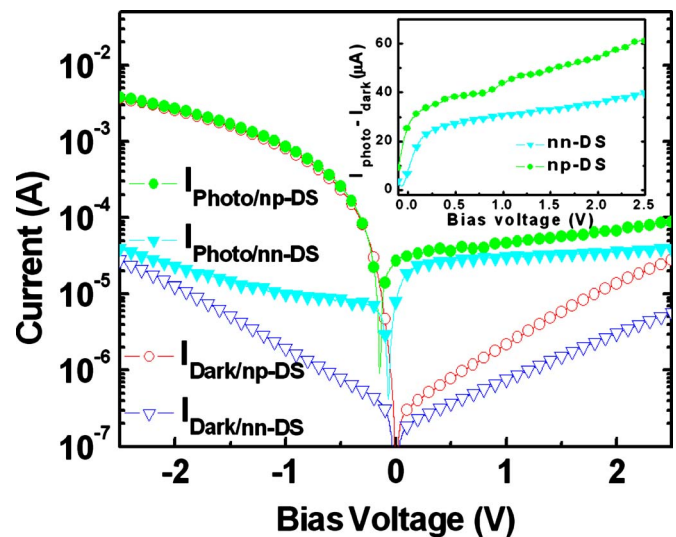


FIG. 4. (Color online) Measured photocurrent at wavelength of $1.55 \mu\text{m}$ for DS-MGM-PD with nn-DS and np-DS. The inset is the photocurrent excluding dark current.

duction of effective hole SBH and, thus, facilitating hole tunneling probability. Simultaneously, the electron current (I_2 and I_3) decreases due to the modulation of effective electron barrier. Since I_1 is the dominant part in the dark current, the PD with pp-DS shows a higher dark current than the PD without DS. The MGM-PD with np-DS shows a dark current of 10^{-6} A at -1 V , which is two to three orders of magnitude lower than that of MGM-PD without DS. It is reported that the NiGe/Ge with As ($1 \times 10^{15} \text{ cm}^{-2}$) segregation can lower the effective electron barrier height up to 0.1 eV.¹¹ Meanwhile, the downward band-bending induced by As DS increases the effective hole SBH^{12,13} and, thus, suppressing the major component of MGM-PD dark current. Among all the structure, the MGM-PD with nn-DS shows lowest dark current. The asymmetry in I - V curves under forward and reverse bias can be attributed to the electrodes width asymmetry.⁷ Figure 3(d) shows the band diagram of MGM with nn-DS, which is similar to the one for DS *n*-MOSFET.^{12,13} The hole current was suppressed due to the increase of effective hole barrier height. In addition, the SB in low potential electrode blocks the thermally generated hole current (I_4).

The dark current comparison of DS-MGM-PDs indicates that hole injection over SB is the major contribution to the dark current and As segregation leads to a crucial role in dark current suppression. The effective hole barrier height of As-segregated NiGe/Ge contact is extracted to be 0.5 eV using the thermionic-emission theory.¹⁴ To study the DS effect on PD's efficiency, the photocurrent of MGM-PDs at a wavelength of $1.55 \mu\text{m}$ was measured. Figure 4 shows the photocurrent and dark current of MGM-PDs with nn-DS and np-DS. The inset of Fig. 4 illustrates the comparison of photon generated current (photocurrent minus dark current) between the two DS strategies. The MGM-PD with np-DS shows 50% higher photocurrent than that of the MGM-PD with nn-DS. In Fig. 2, the MGM-PD with nn-DS shows lowest dark current. The hole SB in low potential side not only decreases the thermally generated hole current (I_4) but also blocks the photon generated hole current. It is interesting to observe that the PD with nn-DS shows a low dark current and a high photocurrent when the inner electrode is positive biased. When inner electrode is negatively biased, the PD

shows a higher dark current but a lower photocurrent. Under light illumination, the photogenerated hole in the nn-DS PD encounters an effective hole barrier created by the dopant segregation of As, as shown in Fig. 3(d). With a positive bias, photogenerated hole is limited by the hole barrier at the outer electrode (wider width). A comparison of the photocurrents under positive and negative biases shows that the PD structure asymmetry may alleviate the SB photocurrent blocking effect. However, even at positive-biased condition, MGM-PD with nn-DS still shows 35% degradation in photocurrent as compared to MGM-PD with np-DS. The DS modulated SB at low potential side causes the degradation of the MSM-PD's photocurrent and must be avoided in device design.

In summary, we demonstrated MGM-PDs on Si substrate with suppressed dark current using dopant-segregation technique. The As segregation in electrode plays a crucial role in dark current suppression. The nn-DS structure shows lowest dark current and photocurrent degradation. The degradation can be alleviated by asymmetry electrode width. The DS-MGM-PD with *n*- and *p*-type dopants segregated separately in two electrodes is the optimal structure for dark current suppression and photocurrent detection.

- ¹L. Colace, G. Masini, F. Galluzzi, G. Assanto, G. Capellini, L. Di Gaspare, E. Palange, and F. Evangelisti, *Appl. Phys. Lett.* **72**, 3175 (1998).
- ²J. F. Liu, D. D. Cannon, K. Wada, Y. Ishikawa, S. Jongthammanurak, D. T. Danielson, J. Michel, and L. C. Kimerling, *Appl. Phys. Lett.* **87**, 011110 (2005).
- ³J. F. Liu, J. Michel, W. Giziewicz, D. Pan, K. Wada, D. D. Cannon, S. Jongthammanurak, D. T. Danielson, and L. C. Kimerling, *Appl. Phys. Lett.* **87**, 103501 (2005).
- ⁴J. Oh, S. K. Banerjee, and J. C. Campbell, *IEEE Photonics Technol. Lett.* **16**, 581 (2004).
- ⁵H. C. Luan, D. R. Lim, K. K. Lee, K. M. Chen, J. G. Sandland, K. Wada, and L. C. Kimerling, *Appl. Phys. Lett.* **75**, 2909 (1999).
- ⁶C. O. Chui, A. K. Okyay and K. C. Saraswat, *IEEE Photonics Technol. Lett.* **15**, 1585 (2003).
- ⁷A. K. Okyay, C. O. Chui, and K. C. Saraswat, *Appl. Phys. Lett.* **88**, 063506 (2006).
- ⁸A. Kinoshita, Y. Tsuchiya, A. Yagishita, K. Uchida, and J. Koga, 2004 Symposium on VLSI Technology, p. 168.
- ⁹K. Ikeda, Y. Yamashita, N. Sugiyama, N. Taoka, and S. Takagi, *Appl. Phys. Lett.* **88**, 152115 (2006).
- ¹⁰T. H. Loh, H. S. Nguyen, C. H. Tung, A. D. Trigg, G. Q. Lo, N. Balasubramanian, and D. L. Kwong, *Appl. Phys. Lett.* **90**, 092108 (2007).
- ¹¹S. Takagi, N. Taoka, S. Nakaharai, K. Ikeda, T. Tezuka, Y. Yamashita, Y. Moriyama, T. Maedal, and N. Sugiyama, in *ECS 210th Meeting, Chicago*, 2007 (unpublished).
- ¹²M. Zhang, J. Knoch, Q. T. Zhao, St. Lenk, U. Breuer, and S. Mantl, in *Proceedings of ESSDERC, France*, 2005 (unpublished).
- ¹³B. Y. Tsui and C. P. Lin, *IEEE Trans. Electron Devices* **52**, 2455 (2005).
- ¹⁴E. H. Rhoderick and R. H. Williams, *Metal-Semiconductor Contacts*, 2nd ed. (Clarendon, Oxford, 1988).